



**AFRL-RX-WP-TP-2012-0369**

**LOW TEMPERATURE SUPERPLASTICITY OF Ti-6Al-4V  
PROCESSED BY WARM MULTIDIRECTIONAL  
FORGING (PREPRINT)**

**S.L. Semiatin  
Metals Branch  
Structural Materials Division**

**G.A. Salishchev, E.A. Kudrjavitsev, and S.V. Zharebtsov  
Belgorod State University**

**July 2012  
Interim**

**Approved for public release; distribution unlimited.**

*See additional restrictions described on inside pages*

**STINFO COPY**

**AIR FORCE RESEARCH LABORATORY  
MATERIALS AND MANUFACTURING DIRECTORATE  
WRIGHT-PATTERSON AIR FORCE BASE, OH 45433-7750  
AIR FORCE MATERIEL COMMAND  
UNITED STATES AIR FORCE**

REPORT DOCUMENTATION PAGE					Form Approved OMB No. 0704-0188	
<p>The public reporting burden for this collection of information is estimated to average 1 hour per response, including the time for reviewing instructions, searching existing data sources, gathering and maintaining the data needed, and completing and reviewing the collection of information. Send comments regarding this burden estimate or any other aspect of this collection of information, including suggestions for reducing this burden, to Department of Defense, Washington Headquarters Services, Directorate for Information Operations and Reports (0704-0188), 1215 Jefferson Davis Highway, Suite 1204, Arlington, VA 22202-4302. Respondents should be aware that notwithstanding any other provision of law, no person shall be subject to any penalty for failing to comply with a collection of information if it does not display a currently valid OMB control number. <b>PLEASE DO NOT RETURN YOUR FORM TO THE ABOVE ADDRESS.</b></p>						
1. REPORT DATE (DD-MM-YY) July 2012		2. REPORT TYPE Technical Paper		3. DATES COVERED (From - To) 1 June 2012 – 1 July 2012		
4. TITLE AND SUBTITLE LOW TEMPERATURE SUPERPLASTICITY OF Ti-6Al-4V PROCESSED BY WARM MULTIDIRECTIONAL FORGING (PREPRINT)				5a. CONTRACT NUMBER In-house		
				5b. GRANT NUMBER		
				5c. PROGRAM ELEMENT NUMBER 62102F		
6. AUTHOR(S) S.L. Semiatin (RXCM) G.A. Salishchev, E.A. Kudrjavitsev, and S.V. Zharebtsov (Belgorod State University)				5d. PROJECT NUMBER 4347		
				5e. TASK NUMBER 20		
				5f. WORK UNIT NUMBER 25100102		
7. PERFORMING ORGANIZATION NAME(S) AND ADDRESS(ES) Metals Branch Structural Materials Division Air Force Research Laboratory, Materials and Manufacturing Directorate Wright-Patterson Air Force Base, OH 45433-7750 Air Force Materiel Command, United States Air Force				8. PERFORMING ORGANIZATION REPORT NUMBER AFRL-RX-WP-TP-2012-0369		
9. SPONSORING/MONITORING AGENCY NAME(S) AND ADDRESS(ES) Air Force Research Laboratory Materials and Manufacturing Directorate Wright-Patterson Air Force Base, OH 45433-7750 Air Force Materiel Command United States Air Force				10. SPONSORING/MONITORING AGENCY ACRONYM(S) AFRL/RXCM		
				11. SPONSORING/MONITORING AGENCY REPORT NUMBER(S) AFRL-RX-WP-TP-2012-0369		
12. DISTRIBUTION/AVAILABILITY STATEMENT Approved for public release; distribution unlimited. Preprint to be submitted to Materials Science Forum.						
13. SUPPLEMENTARY NOTES The U.S. Government is joint author of this work and has the right to use, modify, reproduce, release, perform, display, or disclose the work. PA Case Number and clearance date: 88ABW-2012-2163, 12 April 2012. This document contains color.						
14. ABSTRACT Multidirectional forging has been developed to produce an ultrafine-grain (UFG) microstructure in the two-phase titanium alloy Ti-6Al-4V. A microstructure with a grain size of 135 nm was attained, enabling low-temperature superplasticity (LTSP) at 550 degrees Celsius. A total elongation of 1000% and strain-rate-sensitivity coefficient $m=0.47$ were obtained at the optimal strain rate of $2 \times 10^{-4} \text{ s}^{-1}$ . Important features of the microstructure and superplastic behavior of the alloy are summarized in the present work. It is shown that microstructure evolution during low-temperature deformation plays a key role in superplastic flow behavior.						
15. SUBJECT TERMS low-temperature superplasticity, multidirectional forging, ultrafine grain structure, microstructure evolution						
16. SECURITY CLASSIFICATION OF:			17. LIMITATION OF ABSTRACT: SAR	NUMBER OF PAGES 8	19a. NAME OF RESPONSIBLE PERSON (Monitor) Donna Ballard 19b. TELEPHONE NUMBER (Include Area Code) N/A	
a. REPORT Unclassified	b. ABSTRACT Unclassified	c. THIS PAGE Unclassified				

# Low Temperature Superplasticity of Ti-6Al-4V Processed by Warm Multidirectional Forging

G.A. Salishchev<sup>1,a</sup>, E.A. Kudryavtsev<sup>1,b</sup>, S.V. Zharebtsov<sup>1,c</sup>, S.L. Semiatin<sup>2,d</sup>

<sup>1</sup> Belgorod State University, Pobeda 85, Belgorod 308015, Russia

<sup>2</sup> Air Force Research Laboratory, Materials and Manufacturing Directorate, AFRL/RXLM, Wright-Patterson Air Force Base, OH 45433-7817 USA

<sup>a</sup>[Salishchev@bsu.edu.ru](mailto:Salishchev@bsu.edu.ru), <sup>b</sup>[Kudryavtsev@bsu.edu.ru](mailto:Kudryavtsev@bsu.edu.ru), <sup>c</sup>[ser\\_z@mail.ru](mailto:ser_z@mail.ru), <sup>d</sup>[Lee.Semiatin@wpafb.af.mil](mailto:Lee.Semiatin@wpafb.af.mil)

**Keywords:** Low-temperature superplasticity, Multidirectional forging, Ultrafine grain structure, Microstructure evolution

**Abstract.** Multidirectional forging has been developed to produce an ultrafine-grain (UFG) microstructure in the two-phase titanium alloy Ti-6Al-4V. A microstructure with a grain size of 135 nm was attained, enabling low-temperature superplasticity (LTSP) at 550°C. A total elongation of 1000% and strain-rate-sensitivity coefficient  $m=0.47$  were obtained at the optimal strain rate of  $2 \times 10^{-4} \text{ s}^{-1}$ . Important features of the microstructure and superplastic behavior of the alloy are summarized in the present work. It is shown that microstructure evolution during low-temperature deformation plays a key role in superplastic flow behavior.

## Introduction

Manufacturing methods involving severe plastic deformation and the subsequent mechanical properties of two-phase titanium alloys with an UFG microstructure have been studied extensively during the last two decades [1-5]. Different processes, including rolling, multidirectional forging (MF), equal-channel-angular pressing (ECAP), and high-pressure torsion at low temperatures have been applied to produce UFG microstructures. Recent work has shown that a UFG microstructure with a grain size of 100-150 nm can be produced by MF in the  $\alpha/\beta$  titanium alloy Ti-6Al-4V [3].

The great interest in microstructure refinement is associated with significantly reduced superplastic (SP) forming temperatures by as much as a few hundred degrees [6]. For example, in Ti-6Al-4V with a grain size of 300 nm produced by MF, SP behavior was observed at 600°C and a strain rate of  $5 \times 10^{-4} \text{ s}^{-1}$ ; the total elongation  $\delta$  and strain-rate-sensitivity coefficient  $m$  were 500% and 0.34, respectively [7]. The same alloy with the same grain size produced by ECAP showed  $\delta = 296\%$  and  $m = 0.34$  at 600°C and  $1 \times 10^{-4} \text{ s}^{-1}$  [4]. An increase in the deformation temperature resulted in an enhancement of SP properties. Sheets of Ti-6Al-4V with grain size of 300-400 nm produced by MF and subsequent pack rolling showed  $\delta \approx 800\%$  at 650°C and  $\delta > 1000\%$  at 750°C for a strain rate of  $7 \times 10^{-4} \text{ s}^{-1}$  [2].

A decrease in SP properties at lower temperatures may be expected due to both the natural retardation of diffusion-controlled processes and the increase in the fraction of the  $\alpha$  phase in which diffusion is much slower than that in the  $\beta$  phase [8]. Another factor which may contribute to the decreased  $\delta$  is the propensity for grain growth when the fraction of  $\beta$  phase decreases noticeably.

Despite extensive studies of constitutive behavior during LTSP, detailed microstructure evolution data are known only for 775 and 815°C [9]. The aim of the present work, therefore, was to quantify microstructure evolution and mechanical behavior of Ti-6Al-4V with grain size of 135 nm produced by MF during SP deformation at the extremely low temperature of 550°C.

## Materials and Procedures

The program material consisted of the  $\alpha/\beta$  titanium alloy Ti-6Al-4V with a nominal composition (in weight pct.) of 6.3 Al, 4.1 V, 0.18 Fe, 0.03 Si, 0.02 Zr, 0.01 C, 0.18 O, 0.01 N. It was supplied

in the form of a hot-rolled 40-mm diameter bar with a  $\beta$ -transus temperature of 990°C.

Bulk specimens measuring  $\varnothing 40 \times 60$  mm with a UFG microstructure were produced initially by MF under isothermal conditions [3]. For this purpose, preforms water quenched following beta annealing were worked in the temperature interval of 700-550°C using a hydraulic press equipped with isothermal-forging tooling. The nominal strain rate was  $\sim 10^{-3} \text{ s}^{-1}$ . Following MF, 4-mm-thick rolling preforms were sectioned along the longitudinal axis by electric-discharge machining. To increase microstructure homogeneity and to form a rolling texture before SP tension testing, each plate was rolled to sheet at 475°C under isothermal conditions. The reduction per pass was 5-10%. The total reduction of was  $\sim 50\%$ , thus yielding a final sheet thickness of 2 mm.

Tension specimens with a gage section measuring  $12 \times 3 \times 1.5$  mm were machined from the sheets. Tension tests were performed in an Instron mechanical-testing machine at temperatures between 450 and 600°C with a crosshead speed of 0.05-100 mm/min. The strain rate sensitivity  $m$  was evaluated using either the slope of  $\log \sigma - \log \dot{\epsilon}$  curves or strain-rate-change tests [6]. The apparent activation energy of plastic deformation  $Q$  was calculated from the semi-log dependence of the ultimate tensile strength  $\ln(\sigma/G)$  on the inverse absolute temperature ( $1/T$ ) for  $\dot{\epsilon} = 5 \times 10^{-4} \text{ s}^{-1}$  and  $T = 450\text{-}700^\circ\text{C}$ .

X-ray investigation was carried out using a DRON-3 diffractometer with Cu-K $\alpha$  radiation. The details of structural evolution were determined using a JEOL JEM-2100FX transmission electron microscope (TEM) and a Quanta 600 field-emission-gun scanning-electron microscope (SEM).

## Results and Discussion

**Microstructure Evolution during Annealing.** After MF and rolling (referred to as the initial condition), the microstructure consisted of globular  $\alpha$  and  $\beta$  grains with a mean size of 135 nm (Fig. 1a). Due to microscopic residual stresses, some fragments did not have clear boundaries. A histogram of the grain-size distribution (Fig. 1b) suggested quite good homogeneity of the microstructure. However, a small fraction of grains with a size of 300-400 nm was present.

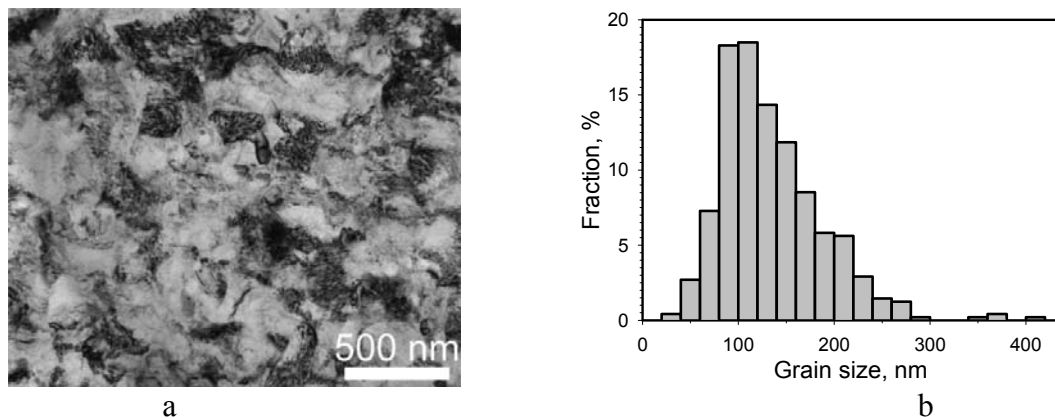


Figure 1 – Microstructure of Ti-6Al-4V in the initial condition (after MF and rolling): (a) TEM bright-field image and (b) grain-size distribution.

Heating to  $T = 550^\circ\text{C}$  resulted in noticeable grain growth; the kinetics of this process depended considerably on soak time (Fig. 2). In the interval of 0 - 4 hours, the grain size increased rapidly; during further soaking at 550°C, the rate of grain growth decreased. After 20 hours, the mean grain size had increased by approximately a factor of three compared to the initial condition (Fig. 2b). A backscattered electron (BSE) image revealed the distribution of the  $\beta$  phase in the microstructure (Fig. 2a). After a short soak time, the  $\beta$  phase appeared in the form of separate particles or thin laths situated between the  $\alpha$  particles (Fig. 2a). An increase in heat treatment time to 20 hours led to coarsening and redistribution of the  $\beta$  particles mainly to triple points. The volume fraction of the  $\beta$  phase (determined by the linear intercept method) was  $\sim 10\%$  in the initial condition and did not change noticeably during annealing.

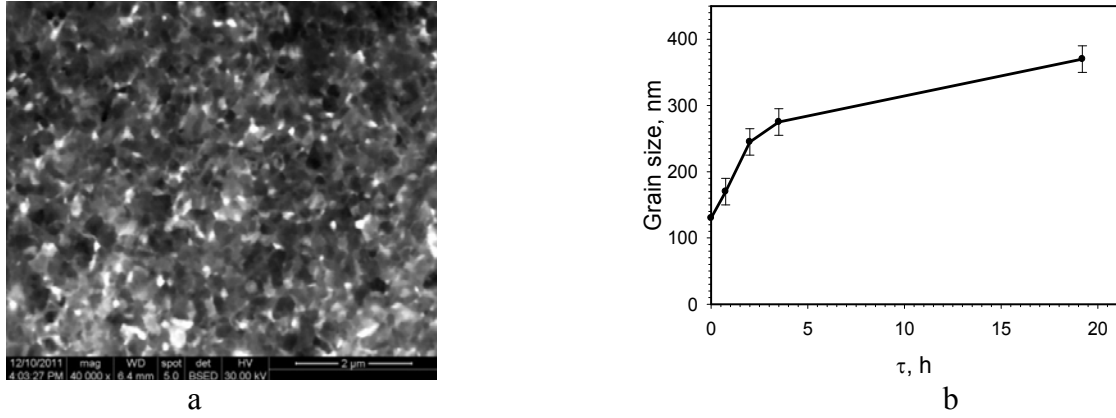


Figure 2 - (a) BSE image of Ti-6Al-4V after annealing at  $T=550^{\circ}\text{C}$  for 0.5 hour and (b) grain size as a function of soak time at  $550^{\circ}\text{C}$ .

**Superplastic Behavior.** Figure 3 shows the mechanical properties of the UFG alloy as a function of temperature and strain rate. An increase in deformation temperature increased the ductility of the alloy and resulted in a marked decrease in flow stress (Fig. 3a). At  $T=550^{\circ}\text{C}$  and  $\dot{\epsilon}=5\times 10^{-4} \text{ s}^{-1}$ , the total elongation  $\delta$  was 640%. A further increase in temperature led to a small increase in  $\delta$ , a trend likely mitigated by the oxidation effect and the formation of alpha case. An examination of specimens strained at different temperatures (Fig. 4a) showed that deformation at  $550^{\circ}\text{C}$  occurred homogeneously with obvious signs of SP flow. The effect of strain rate on the mechanical behavior at  $550^{\circ}\text{C}$  was also typical of that for SP deformation (Fig. 3b). The optimal SP parameters for the UFG alloy were  $\delta=1000\%$  and  $m = 0.47$  at a strain rate of  $2\times 10^{-4} \text{ s}^{-1}$ .

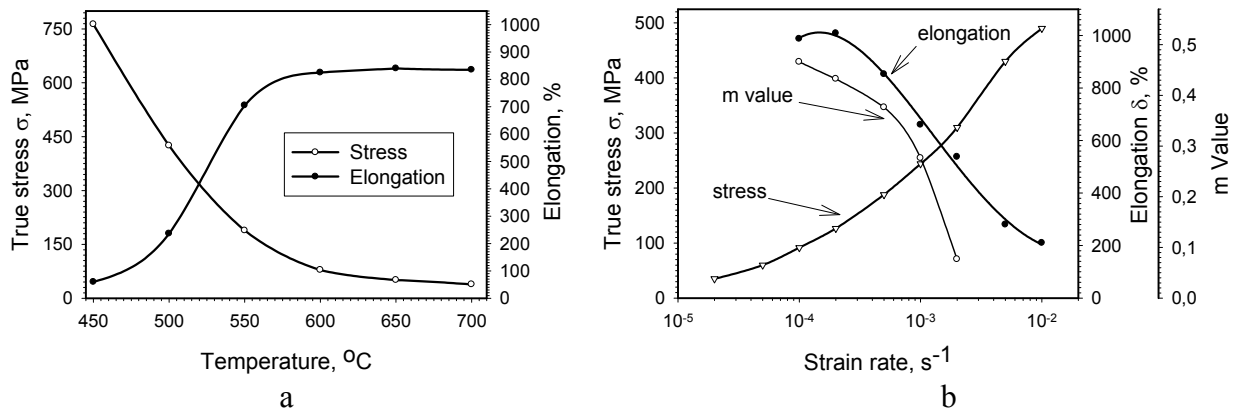


Figure 3 – Mechanical properties of the UFG alloy as a function of (a) deformation temperature for  $\dot{\epsilon}=5 \times 10^{-4} \text{ s}^{-1}$  and (b) strain rate for  $T=550^{\circ}\text{C}$ . The stress level was defined at  $\epsilon \sim 0.2$ .

The shape of the flow curves for the UFG material at  $T=550^{\circ}\text{C}$  (corrected to a constant true strain rate) depended noticeably on strain rate. At  $2\times 10^{-3} \text{ s}^{-1}$ , the flow curve exhibited a peak flow stress at the initial stages of deformation and then near steady-state flow until fracture. A decrease in the strain rate to the optimal value of  $2\times 10^{-4} \text{ s}^{-1}$  changed the mechanical behavior to a marked flow-hardening response suggestive of dynamic coarsening [9]. A similar behavior was observed at the yet lower strain rate of  $2\times 10^{-5} \text{ s}^{-1}$ . In general, such behaviors are typical of SP flow. However, there are large differences in the levels of flow stress. For the optimal condition at  $2\times 10^{-4} \text{ s}^{-1}$ , the flow stress was  $\sim 130 \text{ MPa}$ . This is an order of magnitude higher than that typically observed for high-temperature superplasticity at the same strain rate [6]. The higher flow stresses can be ascribed largely to the marked decrease in the diffusivity at the lower temperatures utilized.

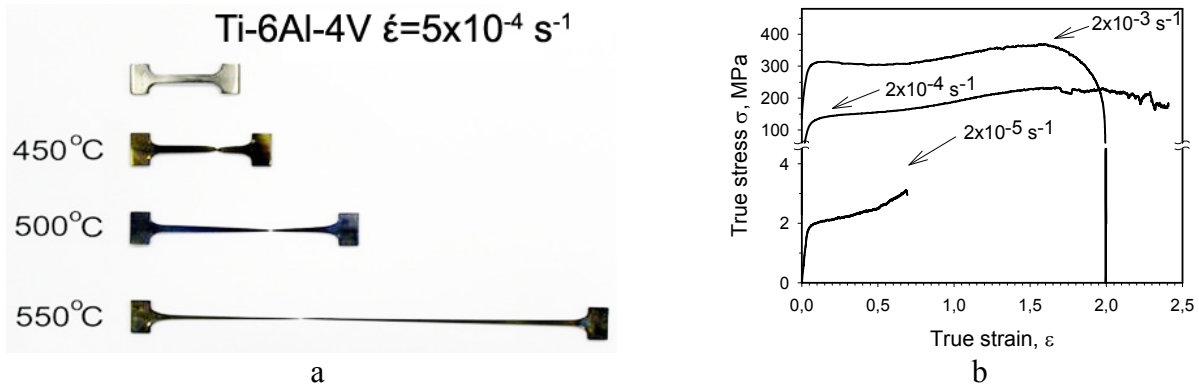


Figure 4 – (a) Macrographs of test specimens of UFG Ti-6Al-4V after SP deformation at different temperatures and a strain rate of  $5 \times 10^{-4} \text{ s}^{-1}$  and (b) true stress- true strain curves for UFG Ti-6Al-4V obtained at  $T = 550^\circ\text{C}$  and various strain rates.

**Apparent Activation Energy of Plastic Deformation.** The activation energy for a specific deformation process can provide insight into the rate-controlling mechanism. Under the optimal parameters of superplasticity,  $Q = 149 \text{ kJ/mol}$  at  $n = 2$  was obtained. In earlier works [4, 10] for the same alloy, a similar values of  $176 \text{ kJ/mol}$  for region II of superplasticity at  $T = 600^\circ\text{C}$  and  $160 \text{ kJ/mol}$  at temperatures between  $650$  and  $955^\circ\text{C}$  were reported.

**Microstructure Evolution.** Microstructure evolution of the UFG alloy at  $T = 550^\circ\text{C}$  as a function of strain and strain rate was quantified. Strain rate can greatly influence microstructure evolution; a decrease in strain rate often results in grain growth. For a strain  $\epsilon = 100\%$ , the mean grain size was found to be  $290 \text{ nm}$  at  $\dot{\epsilon} = 5 \times 10^{-3} \text{ s}^{-1}$ ,  $490 \text{ nm}$  at  $\dot{\epsilon} = 2 \times 10^{-4} \text{ s}^{-1}$ , and  $530 \text{ nm}$  at  $\dot{\epsilon} = 2 \times 10^{-5} \text{ s}^{-1}$ . An increase in strain using the optimal strain rate for superplasticity also resulted in considerable grain growth such that a measurable fraction of grains with a size of the order of  $1400 \text{ nm}$  was observed (Fig. 5a). The plot in Fig 5b further quantifies strain-induced grain growth at  $2 \times 10^{-4} \text{ s}^{-1}$  and  $T = 550^\circ\text{C}$  as compared to that during annealing at  $550^\circ\text{C}$  for equivalent times.

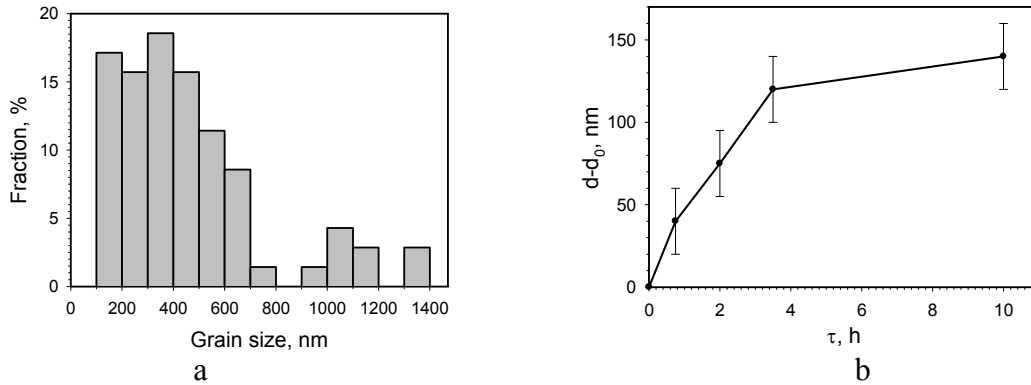


Figure 5 – (a) Grain-size distribution after  $\epsilon = 500\%$  and (b) strain-induced grain growth at  $2 \times 10^{-4} \text{ s}^{-1}$  and  $T = 550^\circ\text{C}$  in comparison with that during annealing for the same time as that needed for a given strain. In (b)  $d$  denotes the mean grain size after a given strain and  $d_0$  is the mean grain size after annealing for the equivalent time.

Under optimal SP conditions, the strain rate sensitivity was determined to be  $m = 0.52$ ,  $0.62$  and  $0.65$  for elongations of  $100$ ,  $200$ , and  $500\%$ , respectively. Consequently, despite considerable grain growth after large plastic strain, SP flow was still observed.

TEM investigation of substructure evolution during SP deformation of the UFG alloy to an elongation of  $100\%$  at  $T = 550^\circ\text{C}$  and various strain rates indicated the presence of dislocations in the  $\alpha$  phase even after slowest strain rate of  $2 \times 10^{-5} \text{ s}^{-1}$ . The dislocation density tended to decrease with a decrease in strain rate. However, the absolute change in comparison to the initial condition was small. The absence of porosity in the specimens deformed to fracture ( $\epsilon = 1000\%$ ) at  $2 \times 10^{-4} \text{ s}^{-1}$  was also noted.

**Texture Evolution.** The evolution of the crystallographic texture during annealing and SP deformation was quite typical [6]. In the initial condition (Fig. 6a), the (0002)  $\alpha$ -phase pole figure consisted of a sharp split texture with basal poles tilted  $\sim 30^\circ$  from the ND toward the TD and slightly split toward the RD direction. Annealing changed neither the intensity nor the location of the poles considerably (Fig. 6b). During SP deformation, the basal poles moved toward the RD direction (Fig. 6c). The intensity of poles decreased slightly with decreasing SP strain rate. An increase in strain from 100 to 500% under the optimal strain rate of  $\dot{\epsilon} = 2 \times 10^{-4} \text{ s}^{-1}$  resulted in the formation of a diffuse pole figure with much lower intensity (Fig. 6d). The Kearn's factor calculated from the pole density [11] for the normal plane of tensile specimens decreased from 0.55 in the initial condition to 0.42 after 500% elongation at  $2 \times 10^{-4} \text{ s}^{-1}$ .

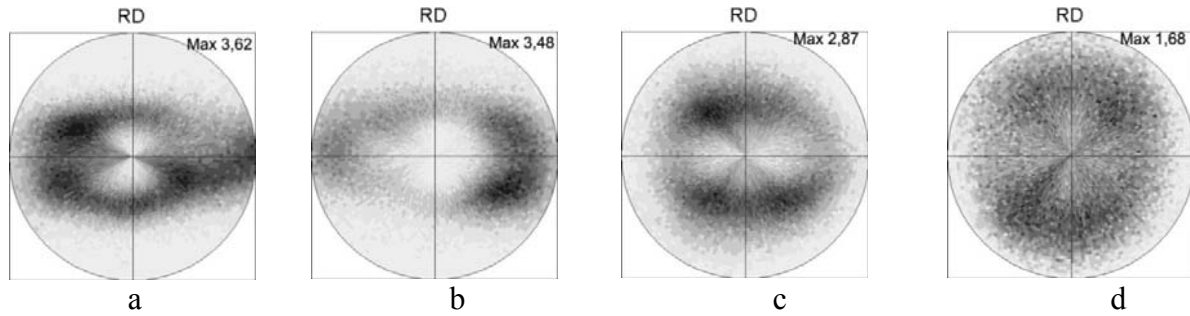


Figure 6 – (0002) $\alpha$  pole figures taken from the normal plane of the plate produced by MF and rolling: (a) In the initial condition and (b) after annealing at 550°C for 0.5 h. (0002) $\alpha$  pole figures measured on tension-specimen gage sections (on the surface corresponding to the normal plane of the initial sheet) after testing at  $\dot{\epsilon} = 2 \times 10^{-4} \text{ s}^{-1}$  to an elongation of (c) 100% or (d) 500%.

## Discussion

UFG Ti-6Al-4V exhibited SP behavior at the extremely low temperature of 550°C. This temperature falls into the interval typically used to age the alloy (i.e., 480-595°C [12]), thus implying reasonable diffusivity. However, a decrease in temperature to 450°C (below the lower bound of this interval) resulted in an increase in flow stress to 760 MPa, a value more than 4 times that at 550°C (170 MPa) (Fig. 3a). The decrease in grain size to 135 nm made possible SP deformation with high values of strain rate sensitivity, uniform and total elongation, and flow hardening as a result of dynamic grain growth/ $\alpha$ -particle coarsening under the optimal conditions. However, some features of the SP behavior are noteworthy.

It is usually thought that SP behavior in Ti-6Al-4V can be expected when the ratio of the  $\alpha/\beta$  volume fractions is close to 1 [6, 12]. This is because (i) grain boundary sliding occurs more readily along interphase boundaries and (ii) microstructure stability is enhanced. A reduction of temperature to 550°C leads to a marked decrease in the fraction of the  $\beta$  phase to  $\sim 10\%$ , thereby decreasing the length of the interphase boundaries and increasing microstructural instability. Indeed, the kinetics of strain-induced grain growth are much faster than those during static annealing (Fig. 5b). In addition, the fact that the tested specimens did not exhibit porosity near the fracture surface at low temperatures appears very unusual, and may be partially rationalized on the basis of grain-coarsening enhanced relaxation of intergranular stresses during SP deformation.

The mechanism of LTSP in UFG Ti-6Al-4V can be deduced based on the value of the apparent activation energy. Although the value obtained here (149 kJ/mol) is slightly lower than that reported for higher-temperature SP (176 and 160 kJ/mol [4, 10]), the difference is not large. Also, the value of activation energy obtained in the present work is similar to that reported in [13] for grain-boundary diffusion in the SP regime from 800 to 950°C for conventional Ti-6Al-4V (189 kJ/mole). Thus, it may be hypothesized that the deformation mechanism for UFG Ti-6Al-4V at lower temperatures is grain-boundary sliding accommodated by grain-boundary diffusion.

The reduction in texture intensity during SP deformation can also be ascribed to grain-boundary sliding and the concomitant randomization effect associated with the rotation of  $\alpha$  particles. The

phenomenon is similar to that observed previously in Ti-6Al-4V [9] and Zn-22%Al [6]. The observed decrease in the Kearn's factor from 0.52 to 0.44 also suggests a weakening of crystallographic texture toward a random one, which would exhibit a Kearn's factor of 0.361 measured for the normal plane of tested specimens (0.333 in a perfectly-random material).

## Summary and Conclusions

1. Superplastic deformation of Ti-6Al-4V with a mean grain size of 135 nm at the extremely low temperature of 550°C was investigated. Using the optimal strain rate of  $2 \times 10^{-4} \text{ s}^{-1}$ , a total elongation of 1000% was obtained with a strain rate sensitivity and flow stress of 0.47 and 130 MPa, respectively.
2. Microstructure observations showed extensive deformation-induced grain growth during SP deformation. The specimens did not have porosity near the fracture surface.
3. The texture weakened considerably during low-temperature SP deformation. Such weakening was mirrored in the values of the Kearn's factor which decreased from 0.52 to 0.44, the latter value approaching that of a random material (i.e., 0.361)
4. The apparent activation energy under the optimal SP conditions was found to be of 149 kJ/mole at  $n=2$  ( $m=0.5$ ) indicating that the dominant deformation mechanism was grain-boundary sliding accommodated by grain-boundary diffusion and possibly matrix-dislocation activity.

## Acknowledgements

This work was supported by Grant № P725 from the Russian Ministry of Science and Education.

## References

- [1] H. Inagaki, Enhanced superplasticity in high strength Ti alloys, *Z. Metallk.* 86 (1995) 643-650.
- [2] G.A. Salishchev et al., Development of Ti-6Al-4V sheet with low temperature superplastic properties, *J. Mater. Proc. Technol.* 116 (2001) 265-268.
- [3] S.V. Zharebtsov et al., Production of submicrocrystalline structure in large-scale Ti-6Al-4V billet by warm severe deformation processing, *Scripta Mater.* 51 (2004) 1147-1151.
- [4] Y.G. Ko et al., Low-temperature superplasticity of ultra-fine-grained Ti-6Al-4V processed by equal-channel angular pressing, *Metall. Mater. Trans.* 37A (2006) 381-391.
- [5] A.V. Sergueeva et al., Superplastic behaviour of ultrafine-grained Ti-6Al-4V alloys, *Mater. Sci. Eng. A323* (2002) 318-325.
- [6] O.A. Kaibyshev: *Superplasticity of Alloys, Intermetallides and Ceramics* (Springer-Verlag, Berlin 1992).
- [7] G.A. Salishchev et al., Submicrocrystalline and nanocrystalline structure formation in materials and search for outstanding superplastic properties, *Mater. Sci. Forum* 170-172 (1994) 121-130.
- [8] Y. Mishin, C. Herzig, Diffusion in the Ti-Al system, *Acta Mater.* 48 (2000) 589-623.
- [9] S.L. Semiatin et al., Plastic flow and microstructure evolution during low-temperature superplasticity of ultrafine Ti-6Al-4V sheet material, *Metall. Mater. Trans.* 41A (2010) 499-512.
- [10] G.A. Sargent et al., Low-temperature coarsening and plastic flow behavior of an  $\alpha/\beta$  titanium billet material with an ultrafine microstructure, *Metall. Mater. Trans.* 39A (2008) 2949-2964.
- [11] G. Wasserman and I. Greven: *Texturen metallischer Werkstoffe* (Springer-Verlag, Berlin 1962).
- [12] M.J. Donachie, Jr.: *Titanium: a Technical Guide* (ASM International, USA 2000).
- [13] A. Arieli, A. Rosen, Superplastic deformation of Ti-6Al-4V, *Metall. Trans.* 8A (1977) 1591-1596.